

# Dynamic Jahn-Teller effect in the EPR spectrum of $\text{Ni}^{1+}$ and $\text{Ni}^{3+}$ in magnesium oxide

A. Schoenberg and J. T. Suss

*Solid State Physics Department, Israel Atomic Energy Commission, Soreq Nuclear Research Centre, Yavne, Israel*

Z. Luz

*Isotope Department, The Weizmann Institute of Science, Rehovot, Israel*

W. Low

*Microwave Division, The Racah Institute of Physics, The Hebrew University, Jerusalem, Israel*

(Received 25 June 1973; revised manuscript received 18 September 1973)

An electron-spin-resonance study of the dynamic Jahn-Teller effect in  $\text{Ni}^{1+}$  and  $\text{Ni}^{3+}$  in MgO at liquid-helium temperature is reported. For both ions the spectra arise from strain-split ground vibronic doublets, with a small admixture of an excited singlet. From the anisotropy of the linewidth it follows that the symmetry of this singlet is  $A_2$  for  $\text{Ni}^{1+}$  and  $A_1$  for  $\text{Ni}^{3+}$ .

## INTRODUCTION

It is well known that ions possessing orbitally degenerate electronic ground states are subject to the Jahn-Teller (JT) effect. This effect has been studied extensively in a number of transition-metal ions.<sup>1-4</sup> Most of these studies are concerned with  $d^1$  and  $d^9$  configurations, for which examples were presented for both the static and the dynamic cases, and more recently also for the intermediate range.<sup>5-8</sup> Much less work has been done on  $d^7$  ions, and all of the published cases for such ions deal with the static JT effect only.<sup>1-4,9</sup>

In the present work we report an EPR study of  $\text{Ni}^{1+}$ ,  $\{t_{2g}^6 e_g^3\}^2 E_g$  and  $\text{Ni}^{3+}$ ,  $\{t_{2g}^6 e_g^1\}^2 E_g$  ions in MgO. These systems were investigated previously<sup>10,11</sup> down to liquid-helium temperatures; however, for both cases only a single isotropic line, ascribed to a dynamic JT effect, was reported. In the crystals studied in the present work an anisotropic doublet, in addition to the isotropic line, appeared in the spectra of both ions at low temperature. Analysis of the spectra shows that the anisotropic lines originate from a nearly isolated ground vibronic doublet split by large random strains, while the isotropic lines result from fast averaging of the anisotropic spectra. In addition, it is shown that the ground vibronic doublet contains a small admixture of an excited vibronic singlet state and it was possible to determine the symmetry of this state for both ions.  $\text{Ni}^{3+}$  is the first example of such a dynamic effect for a  $d^7$  low-spin configuration.

## EXPERIMENTAL

Two types of MgO crystals were used: (i) crystals grown in our laboratory by evaporation from  $\text{PbF}_2$  flux,<sup>12</sup> and (ii) commercial crystals (Semi-elements Inc.) grown by the arc-fusion method.  $\text{Ni}^{1+}$  and  $\text{Ni}^{3+}$  occupy substitutional octahedral sites

in the same environment in the crystals. They were obtained from  $\text{Ni}^{2+}$  impurity by irradiation at room temperature. It may be of interest to note that in crystals grown from flux in an atmosphere of oxygen, only a weak  $\text{Ni}^{3+}$  signal was obtained. The crystals contained also other paramagnetic centers such as  $V$  centers,  $\text{Mn}^{2+}$ ,  $\text{Fe}^{3+}$ ,  $\text{Cr}^{3+}$ , etc.

EPR measurements were performed at 4.2 °K (and some preliminary measurements also at 1.8 °K), on an X-band Varian spectrometer. The magnetic field was calibrated by a proton-resonance probe and by the hyperfine structure of  $\text{Mn}^{2+}$  impurity.<sup>13</sup>

## RESULTS AND DISCUSSION

Typical first derivative EPR spectra at 4.2 °K in flux-grown MgO crystal, at two orientations of the magnetic field, are shown in Fig. 1. For each of the two ions one observes two types of coexisting spectra, an isotropic line (already reported previously<sup>10,11</sup>) and an anisotropic doublet whose components are located very nearly symmetrically about the corresponding isotropic lines. The  $g$  values for the two isotropic lines are

$$g_{\text{iso}} = 2.2391 \pm 0.0006 \text{ for } \text{Ni}^{1+},$$

$$g_{\text{iso}} = 2.1685 \pm 0.0008 \text{ for } \text{Ni}^{3+}.$$

The angular dependence of the spectra in the (100) and (110) planes are shown in Fig. 2. The largest separation of the doublet components occurs when the magnetic field is parallel to the [100] and equivalent directions, while along [111] the doublets coalesce with the corresponding isotropic lines. The doublet components are asymmetric and exhibit a powderlike shape, characteristic of a random-strain-broadened envelope.<sup>14</sup> Their widths range between 6 and 15 G for  $\text{Ni}^{3+}$  and between 8 and 20 G for  $\text{Ni}^{1+}$ . The isotropic lines are

more symmetric; they have nearly isotropic widths (about 9 G for both ions), but their intensity is strongly anisotropic. It is largest close to the [111] direction, whereas along the [100] and equivalent directions their intensity is much reduced.

This behavior is typical of a strain-split vibronic doublet state. The quantitative interpretation of such spectra has been discussed by several authors.<sup>2-14</sup> The anisotropic doublets correspond to extrema in the envelope spectrum, while the isotropic lines result from dynamic averaging of the central part of this envelope. The angular dependence of the resonance fields,  $H^\pm$ , of the components of the anisotropic doublet can be described to first order by<sup>14</sup>

$$H^\pm = (h\nu/g_1 \mu_B) [1 \mp (qg_2/g_1)f] \quad (1)$$

where  $f \equiv [1 - 3(l^2 m^2 + m^2 n^2 + n^2 l^2)]^{1/2}$ ,  $g_1$  and  $g_2$  are components of the  $g$  tensor,  $q$  is a "reduction factor" and  $l$ ,  $m$ , and  $n$  are direction cosines of the magnetic field relative to the cubic axes. The  $\pm$  signs in Eq. (1) refer to Zeeman transitions within the strain-split vibronic doublet eigenstates<sup>4,14</sup>,

$$|+\rangle = \sin \frac{1}{2} \omega |\theta_{\text{vib}}\rangle + \cos \frac{1}{2} \omega |\epsilon_{\text{vib}}\rangle, \quad (2a)$$

$$|-\rangle = \cos \frac{1}{2} \omega |\theta_{\text{vib}}\rangle - \sin \frac{1}{2} \omega |\epsilon_{\text{vib}}\rangle, \quad (2b)$$

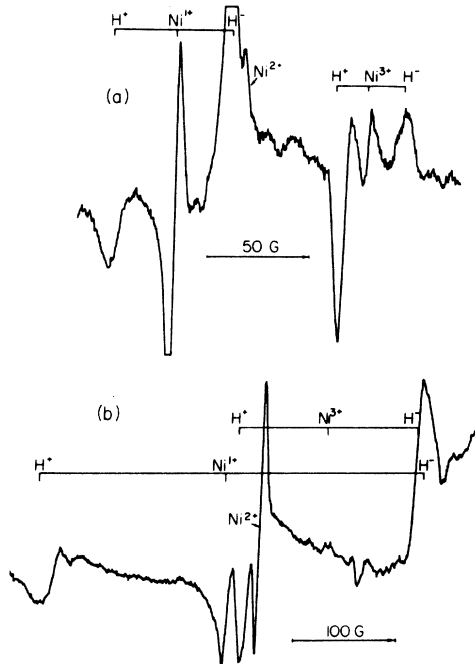


FIG. 1. EPR spectra (first derivative) of  $Ni^{1+}$  and  $Ni^{3+}$  in flux-grown MgO crystals at 4.2°K. (a)  $\vec{H}_{dc}$  is in the (110) plane, 48° from the [001] direction. (b)  $\vec{H}_{dc}$  || [001].

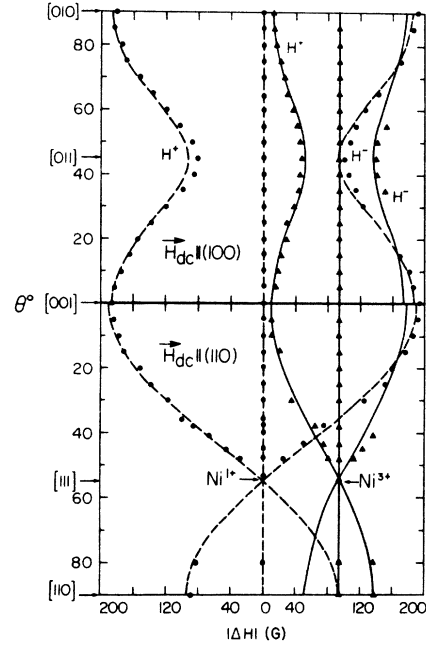


FIG. 2. Angular variation of the  $Ni^{1+}$  and  $Ni^{3+}$  spectra in the (110) and (100) planes. The points are experimental, while the continuous curves are calculated from Eq. (1) using the best-fit parameters given in the text.

where

$$\sin \omega = \frac{1}{2} \sqrt{3} (l^2 - m^2) / f \quad (3a)$$

and

$$\cos \omega = \frac{1}{2} (3n^2 - 1) / f \quad (3b)$$

Equation (1) applies if the vibronic doublet is well separated from the first excited singlet state. A best-fit analysis of the experimental points in Fig. 2 showed that for both ions  $g_1 = g_{100}$  and using Eq. (1) gave the following results for  $qg_2$ :

$$qg_2 = 0.06 \text{ for } Ni^{3+}, \quad (4a)$$

$$qg_2 = 0.145 \text{ for } Ni^{1+}. \quad (4b)$$

The assignment  $H^+$  and  $H^-$  in Fig. 2 is arbitrary. In fact, as will be discussed later on each line has contributions from both components of the strain-split doublet [Eq. (2)]. In the analysis of the  $Ni^{3+}$  results, only the  $H^+$  points were used, since the  $H^-$  component was in many orientations broadened and obscured by other lines in the spectrum.

To obtain values for  $q$  from results in Eqs. (4),  $g_2$  must be known. It can, in principle, be calculated from crystal-field theory. For the orbital doublet  $E_g$  one finds<sup>15</sup>

$$g_1 = \frac{1}{3} (g_{\parallel} + 2g_{\perp}), \quad (5a)$$

$$g_2 = \mp \frac{2}{3} (g_{\parallel} - g_{\perp}) \quad (5b)$$

where the upper (lower) sign applies to the  $\theta(\epsilon)$  component. It is generally the case that for an "E<sub>g</sub> hole" ( $d^9$ ) the ground orbital state is  $\epsilon$  while for an "E<sub>g</sub> electron" ( $d^7$ ) it is  $\theta$ .<sup>16</sup> Crystal-field theory gives<sup>17</sup> for  $d^9$ ,

$$g_{\parallel}(\epsilon) = g_s \quad (6a)$$

$$g_{\perp}(\epsilon) = g_s - 6\lambda/\Delta \quad (6b)$$

and, thus,

$$g_2(\epsilon) = g_1 - g_s \quad (7)$$

Therefore for Ni<sup>1+</sup>

$$q = qg_2/g_2 = qg_2/(g_1 - g_s) = 0.6 \quad (8)$$

For Ni<sup>3+</sup> the situation is more complicated since for  $d^7$  ions actual values of the crystal-field parameters must be known. In this case we have<sup>18,19</sup>

$$g_{\parallel}(\theta) = g_s + 2\zeta^2/\delta^2 \quad (9a)$$

$$g_{\perp}(\theta) = g_s + 2\zeta^2/\delta^2 + 3\zeta/E \quad (9b)$$

where

$$1/E = 1/E_3 + 1/E_4 + 0.38(1/E_3 - 1/E_4) \quad (10)$$

and  $\delta$ ,  $E_3$ , and  $E_4$  are the energy differences as explained in Ref. 18. (Note that  $\zeta$  is the spin-orbit coupling constant for a single  $d$  electron, while  $\lambda$  is that for the <sup>2</sup>D term.) Thus, from Eqs. (5) and (9),

$$g_1(\theta) = g_s + 2\zeta/E + 2\zeta^2/\delta^2 \quad (11a)$$

$$g_2(\theta) = 2\zeta/E \quad (11b)$$

To obtain  $E$  and  $\delta$  the following procedure was adopted. Using Tanabe-Sugano diagrams for  $d^7$  ions,<sup>20</sup> an approximate relation between  $1/E$  and  $\delta$  in terms of the Racah parameter  $B$  can be obtained as follows:

$$\frac{1}{E} = \frac{1}{1520B} \left[ 92.4 - 3.5 \frac{\delta}{B} - 0.12 \left( \frac{\delta}{B} \right)^2 \right] \quad (12)$$

On the other hand,  $1/E$  can be expressed in terms of  $\delta$  and  $\zeta$  using Eq. (11a) and the experimental result for  $g_1$ . Thus assuming numerical values for  $B$  and  $\zeta$ , results for  $E$  (and  $\delta$ ) and thus for  $q$  may be obtained as follows:

$$q = qg_2/g_2 = qg_2/(2\zeta/E) \quad (13)$$

We will compute  $q$  for two sets of values of  $B$  and  $\zeta$ : (i) Taking  $B = 971 \text{ cm}^{-1}$ , the point-charge crystal-field-model value<sup>20</sup> and the single- $d$ -electron spin-orbit coupling constant<sup>19</sup>  $\zeta = 700 \text{ cm}^{-1}$ , one obtains  $E = 18200 \text{ cm}^{-1}$ ,  $\delta = 2950 \text{ cm}^{-1}$ , and using Eq. (13)

$$q = 0.78 \quad .$$

(ii) Introducing covalency by using reduced values<sup>18,19,21</sup> of  $B$  ( $660 \text{ cm}^{-1}$ ) and  $\zeta$  ( $520 \text{ cm}^{-1}$ ) gives  $E = 14000 \text{ cm}^{-1}$ ,  $\delta = 3400 \text{ cm}^{-1}$ , and, thus,

$$q = 0.67 \quad .$$

The results for  $q$  for both ions correspond to the moderate JT coupling region, i. e.,  $E_{JT} \approx \hbar\omega_E$ , where  $\omega_E$  is the frequency of the  $E$  mode. For Ni<sup>3+</sup> this result is consistent with previous independent estimates of  $E_{JT} \approx 325 \text{ cm}^{-1}$ <sup>22</sup> and the commonly used value for  $\hbar\omega_E$  ( $300\text{--}400 \text{ cm}^{-1}$ ) in MgO.<sup>23,24</sup>

Although the general fit in Fig. 2 is quite satisfactory, there are, in many orientations, systematic deviations from Eq. (1). These deviations cannot be explained by second-order correction to this equation.<sup>14</sup> It is however quite possible that they arise from the interaction with an excited low-lying singlet state. That such an interaction indeed exists is supported by the anisotropy of the linewidth discussed below.

As mentioned previously, the linewidth of the doublet components varied with the orientation of the magnetic field. In fact for both ions the width of the two components differed significantly in many orientations. For example, in the (110) plane the lines labeled  $H^-$  for Ni<sup>3+</sup> and  $H^+$  for Ni<sup>1+</sup> were broader than their corresponding partners (Fig. 1). This effect was first discussed by Chase<sup>5</sup> and explained in terms of selective strain-induced mixing of the excited singlet into the ground doublet.

As indicated above, each anisotropic line has contributions from both states of the strain-split doublet  $|+\rangle$  and  $|-\rangle$ . In the (110) plane  $\omega$  is either 0 or  $\pi$  and from Eq. (2) they become pure vibronic states. In fact, since for both the Ni<sup>3+</sup> and Ni<sup>1+</sup> ions  $g_1$  and  $g_2$  are positive<sup>18</sup> [See Eqs. (5), (6), and (11)], the lines labeled  $H^+$  and  $H^-$  in Figs. 1 and 2 correspond, respectively, to  $\epsilon_{vib}$  and  $\theta_{vib}$ . (To see this, it is sufficient to consider Eqs. (1) and (2) along the [001] direction and note that  $\omega = 0$  corresponds to  $f = 1$ , and  $\omega = \pi$  corresponds to  $f = -1$ .) The matrix form of the general Hamiltonian within the vibronic states [ $\theta_{vib}$ ,  $\epsilon_{vib}$ ,  $A_1$  (or  $A_2$ )] is given in Table I.<sup>2,5</sup> For the specific case of strain Hamiltonian,  $G_e$  for the sites contributing to the  $H^+$  lines in the (110) plane vanishes. Thus from Table I,  $\theta_{vib}$  can only mix with  $A_1$ , while  $\epsilon_{vib}$  can only mix with  $A_2$ . This mixing will result in broadening of one of the doublet components, i. e., that one having the right transformation properties to mix with the excited singlet. Comparison with the experimental results shows that for Ni<sup>3+</sup> the low-lying singlet is  $A_1$  while for Ni<sup>1+</sup> it is  $A_2$ . This result also fixes the sign of the "warping" parameter  $\beta$  as positive for both ions.<sup>16</sup> The physical meaning of this is that the JT effect in both cases

TABLE I. General Hamiltonian within the vibronic states [ $\theta_{\text{vib}}$ ,  $\epsilon_{\text{vib}}$ ,  $A_1$  (or  $A_2$ )]. Here  $r$ ,  $r'$  (and  $q$ ) are "reduction parameters" and the  $G$ 's are components of the external forces.

$A_1(A_2)$	$\theta_{\text{vib}}$	$\epsilon_{\text{vib}}$
$3\Gamma + G_1$	$rG_\theta(r'G_\epsilon)$ $G_1 - qG_\theta$	$rG_\epsilon(-r'G_\theta)$ $qG_\epsilon$ $G_1 - qG_\theta$

stabilizes an "elongated octahedron" distortion. This will put the unpaired electron in  $\text{Ni}^{1+}$  into a  $d_{x^2-y^2}$  orbital, while in  $\text{Ni}^{3+}$  it will go into a  $d_{z^2}$  orbital. These results were assumed in deriving the  $g$  values in Eqs. (6) and (9).

The perturbation mixing of an excited singlet into the ground vibronic doublet results also in a small shift of the  $H^\pm$  lines. However, our experimental accuracy was not sufficient for a quantitative analysis of this effect.

Finally, as mentioned in the experimental section, some measurements were also performed on  $\text{MgO}$  crystals grown by the arc-fusion method. In these crystals the anisotropic doublet is only observed at temperatures lower than 4.2 °K, indicating that in these crystals the dynamic averaging rate is higher than in the corresponding crystals grown from the flux. From the general appearance of the EPR spectra of other paramagnetic impurities it seems that the flux-grown crystals are more strained than those obtained by the arc-fusion method. We may therefore rule out the "direct process" as the mechanism for the dynamic averaging (which according to theory<sup>2</sup> is proportional to the cube power of the strain). This problem is currently being investigated.

#### ACKNOWLEDGMENTS

Helpful discussions with Professor R. Englman, Dr. B. Halperin, and A. Raizman are gratefully acknowledged.

- <sup>1</sup>M. D. Sturge, *Solid State Physics*, edited by F. Seitz and D. Turnbull (Academic, New York, 1967), Vol. 20, p. 91.
- <sup>2</sup>F. S. Ham, in *Electron Paramagnetic Resonance*, edited by S. Geschwind (Plenum, New York, 1972), p. 1.
- <sup>3</sup>R. Englman, *The Jahn-Teller Effect in Molecules and Crystals* (Wiley, New York, 1972).
- <sup>4</sup>A. Abragam and B. Bleaney, *Electron Paramagnetic Resonance of Transition Ions* (Oxford U. P., Oxford, England, 1970), Chap. 21.
- <sup>5</sup>L. L. Chase, *Phys. Rev. B* 2, 2308 (1970).
- <sup>6</sup>L. A. Boatner, R. W. Reynolds, M. M. Abraham, and Y. Chen, *Phys. Rev. Lett.* 31, 7 (1973).
- <sup>7</sup>R. W. Reynolds, L. A. Boatner, M. M. Abraham, and Y. Chen, *Bull. Am. Phys. Soc.* 18, 448 (1973).
- <sup>8</sup>A. O. Barksdale and T. L. Estle, *Bull. Am. Phys. Soc.* 18, 448 (1973).
- <sup>9</sup>J. T. Suss, A. Raizman, S. Szapiro, and W. Low, *J. Mag. Res.* 6, 438 (1972).
- <sup>10</sup>W. Low and J. T. Suss, in *Electron Diffraction and the Nature of Defects in Crystals* (Pergamon, New York, 1966), p. II B-1.
- <sup>11</sup>J. W. Orton, P. Auzins, J. H. E. Griffiths, and J. E. Wertz, *Proc. Phys. Soc. Lond.* 78, 554 (1961); U. T.

- Höchli, K. A. Müller, and P. Wysling, *Phys. Lett.* 15, 5 (1965).
- <sup>12</sup>A. Schoenberg, J. T. Suss, S. Szapiro, and Z. Luz, *Phys. Rev. Lett.* 27, 1641 (1971).
- <sup>13</sup>C. Y. Huang, R. S. Kent, and S. A. Marshall, *Phys. Rev. B* 7, 552 (1973); W. M. Walsh, Jr., J. Jeener, and N. Bloembergen, *Phys. Rev.* 139, A1338 (1965).
- <sup>14</sup>J. R. Herrington, T. L. Estle, and L. A. Boatner, *Phys. Rev. B* 3, 2933 (1971).
- <sup>15</sup>Reference 4, Sec. 21.3
- <sup>16</sup>Reference 3, Table 3.2 and p. 139.
- <sup>17</sup>Reference 4, Table 7.22.
- <sup>18</sup>K. A. Müller, W. Berlinger, and R. S. Rubins, *Phys. Rev.* 186, 361 (1969).
- <sup>19</sup>B. Lacroix, U. Höchli, and K. A. Müller, *Helv. Phys. Acta* 37, 627 (1964).
- <sup>20</sup>Y. Tanabe and S. Sugano, *J. Phys. Soc. Jap.* 9, 753, 766 (1954).
- <sup>21</sup>D. M. Hannon, *Phys. Rev.* 164, 366 (1967).
- <sup>22</sup>P. Wysling, U. Höchli, and K. A. Müller, *Helv. Phys. Acta* 37, 629 (1964).
- <sup>23</sup>Reference 3, Table 7.6.
- <sup>24</sup>F. S. Ham, *Phys. Rev. B* 4, 3854 (1971).